Tri-axial Core Design of a Distribution System Class HTS Power Cable

Sung-Kyu Kim[1], Sun-Kyoung Ha[1], Minwon Park[1], In-Keun Yu[1],
Sangjin Lee[2] and Kideok Sim[3]

[1]*Changwon National University, Changwon 641-773 Republic of Korea*
[2]*Uiduk University, Gyeongju 780-713 Republic of Korea*
[3]*Korea Electrotechnology Research Institute, Changwon 641-120 Republic of Korea*
yuik@changwon.ac.kr

Abstract

A tri-axial HTS power cable has been proposed and developed to reduce the number of HTS wires because it has copper shield instead of HTS shield. However, it has a drawback which is an inherent imbalance problem due to an asymmetry configuration in the cable.

The authors designed a 22.9 kV/50 MVA class tri-axial HTS cable. The inherent imbalance problem of the three-phase currents in the tri-axial HTS power cable has been minimized through the adjustment of pitches and radii of each layer. An FEM analysis program and a power system analysis program were used to analyze the characteristics of the designed tri-axial HTS power cable. The AC loss and magnetic characteristics of the designed cable were analyzed according to magnitude of operating currents. The design results of the tri-axial HTS power cable are discussed in detail.

Keywords: *AC loss, Balanced three phase distribution, HTS cable, Tri-axial cable*

1. Introduction

High temperature superconducting (HTS) power cables have been intensively developed as potential cables for urban areas because of extremely low power loss and compactness compared with conventional copper cables [1]. Most of the developed HTS cables have been a coaxial design, which requires several layers of HTS wire to compose not only the forward superconducting path, but a superconducting return path so that external magnetic fields are virtually eliminated. To obtain three phases, three single-phase cables can be arranged adjacently in three separate cryostats or triangularly in a single cryostat [2].

The configuration of tri-axial has a noteworthy material advantage because the external magnetic fields are small due to the vector sum of the three current-carrying phases; therefore, it is possible to eliminate the need for a superconducting return path of each phase and to reduce the amount of HTS wire by half. Also, the total area of cryogenic surface is reduced in the tri-axial configuration, thereby reducing the cryogenic system capacity required to adequately cool the cable. These material and cryogenic advantages, coupled with its compact size, could make the tri-axial cable an interesting prospect for power utilities with an expanding power capacity and limited space of power corridors [3]. However, there is an inherent imbalance in the three-phase currents in the tri-axial cable due to differences in radii of the three concentric phases. The imbalance of the currents causes additional loss and a large leakage field in the cable, and deteriorates the electric power quality [4].

In this paper, several basic parameters of the tri-axial HTS cable, such as radius of each layer, insulation thickness, and the amount of HTS wire, are designed. To resolve the inherent imbalance in the three-phase currents, inductances and capacitances of the tri-axial HTS cable were calculated by electromagnetic formulas. To model the induced shield and phase imbalance currents, an equivalent electric circuit was modeled for the simulation using power system computer aided design/electromagnetic transient including DC (PSCAD/EMTDC). As a result, the tri-axial HTS cable core was designed and its AC loss and electro-magnetic characteristics were analyzed using finite elements method (FEM) software. The design results of the tri-axial HTS cable are compared with the same class triad co-axial HTS cable and the effectiveness of the tri-axial HTS cable is discussed in detail. Compared with the triad co-axial HTS cable of 22.9 kV, 50 MVA [7], the designed tri-axial HTS cable core has the advantage of using only 56% of the number of HTS wires because the HTS shield doesn't exist.

2. Design of the Tri-axial HTS Power Cable

2.1. Design Parameters

The 22.9 kV/50 MVA class tri-axial HTS cable is designed for power grid application. As shown in Figure 1, the tri-axial HTS cable consists of a single phase conductor layer per phase with the YBCO HTS wire which has 4 mm width and 0.2 mm thickness and a shield layer with the copper wire. The operating current of each phase in the tri-axial HTS cable is 1260 Arms and the designed DC critical current of each phase is 2800 A at the 77 K, respectively. The designed basic parameters are shown in Table 1. In this design, a different critical current of HTS wire in each phase is used for the balance of the critical current in each phase.

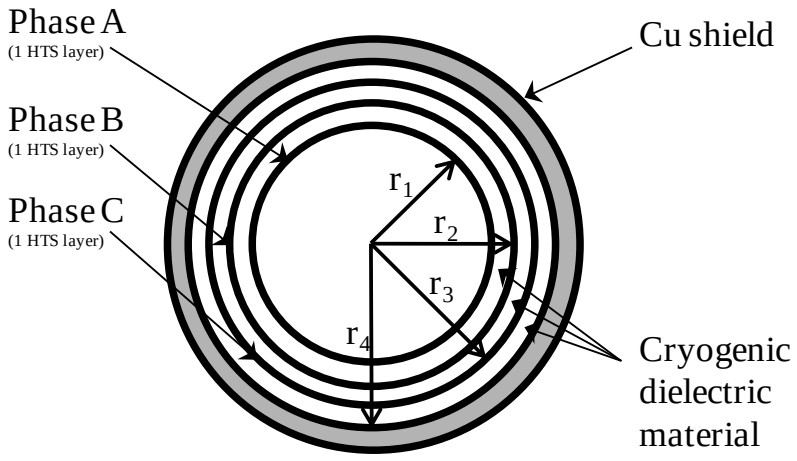

Figure 1. Cross-section of the Tri-axial HTS Cable Showing the Three-phase HTS Conductor Layer and the Copper Shield

Table 1. The Basic Parameters of the Tri-axial HTS Cable

Parameters	Value	Parameters	Value
Voltage / Capacity	22.9 kV / 50 MVA	Insulation thickness	4 mm(PPLP)
Operating current	1260 A_{rms}	Radius of each phase	15 / 19 / 23 mm
DC critical current	2800 A@77 K, self-field	Number of wire	22/ 28/ 34
HTS wire	YBCO wire / RABiTS type	Critical current of each wire	127 / 100 / 82 A @77 K
Gap between wires	0.2 mm	Twist pitch	340 / 220 / 145 mm

2.2. Cable Inductances & Capacitances

When the tri-axial HTS cable is sufficiently short to be approximated by an impedance circuit, the impedance of the cable is mostly the reactance components. For this reason, if the reactance of each phase is the same, current distribution of the cable is balanced. However, it is hard to equalize the reactance of each phase because reactance of each phase depends on the structure and twist pitch of the cable. The inductances of the tri-axial HTS cable consist of two components by tangential and axial magnetic fields. The external inductance caused by tangential fields is due to the magnetic flux external to the phase conductor. The internal inductance caused by axial fields is due to the magnetic flux internal to the phase conductor. The resulting self-inductances per unit length, L_{self}, were found by calculating the enclosed magnetic field energy of each phase.

$$L_{self} = \mu_0 \frac{\pi\, r_i^2}{L_{pi}^2} + \mu_0 \frac{1}{2\pi} \ln\left(\frac{r_s}{r_i}\right) \tag{1}$$

where, r_s is the shield radius, r_i is the each phase radius, μ_0 is the permeability of free space, and L_{pi} is the twist pitch of each phase.

The mutual-inductances between an inner layer i and an outer layer j, M_{ij}, were found by calculating stored magnetic field energy between two phases.

$$M_{ij} = M_{ji} = a_i a_j \mu_0 \frac{\pi\, r_i^2}{L_{pi} L_{pj}} + \mu_0 \frac{1}{2\pi} \ln\left(\frac{r_s}{r_j}\right) \tag{2}$$

where, i and j are not equal, a_i and a_j are direction of twist pitch of each phase.

The capacitances of the tri-axial HTS cable between phases are determined by the structure of the cable as shown in Figure 2(a). The phases are denoted by a, b, and c from the center to the outside. The outermost copper shield layer is grounded. The phase radii are denoted by r_a, r_b, r_c, and r_s, respectively. In such a structure, the phase a potential is screened electrostatically from the phase c and the copper shield by way of the phase b; on the other hand the phase b potential is screened electrostatically from the copper shield by way of the phase c. The capacitances of the cable can be shown in Figure 2(b), (c). The capacitances of the cable were found by calculating the partial capacitance between phases.

$$\begin{pmatrix} I_a \\ I_b \\ I_c \end{pmatrix} = j\omega \begin{pmatrix} C_{ab} & -C_{ab} & 0 \\ -C_{ab} & C_{ab}+C_{bc} & -C_{bc} \\ 0 & -C_{bc} & C_{bc}+C_{cs} \end{pmatrix} \begin{pmatrix} V_a \\ V_b \\ V_c \end{pmatrix}, \qquad C_{ij} = \frac{2\pi\varepsilon_r\varepsilon_0}{\ln\left(\frac{r_j}{r_i}\right)}, \quad \left(where \quad j > i\right) \tag{3}$$

where, r_i is the radius of the inner phase, r_j is the radius of the outer phase, ε_0 is the permittivity of the free space, and ε_r is the relative permittivity of the dielectric material.

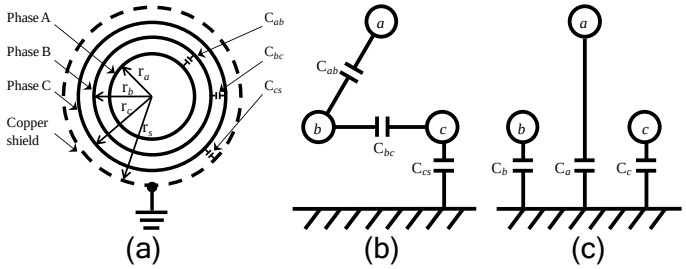

Figure 2. (a) The Structure of the Tri-axial HTS Cable; (b) the Partial Capacitance of the Tri-axial HTS Cable; (c) the Working Capacitance of the Tri-axial HTS Cable

3. Simulations and the Results

3.1. Equivalent Circuit Model

The tri-axial HTS cable was modeled with a lumped-constant circuit to analyze the imbalance of three-phase currents using PSCAD/EMTDC. The equivalent circuit model consists of a three-phase voltage sources, three inductances, three capacitances, and a 50 MW load. This circuit is analyzed to confirm the variation of line to line voltage and three-phase current along cable length in steady state when the cable is connected to a three-phase balanced source with an effective line to line voltage of 22.9 kV. The imbalance of three-phase currents is about 0.09% and the imbalance of three-phase line to line voltage is about 0.03% on the load side at 10 km length.

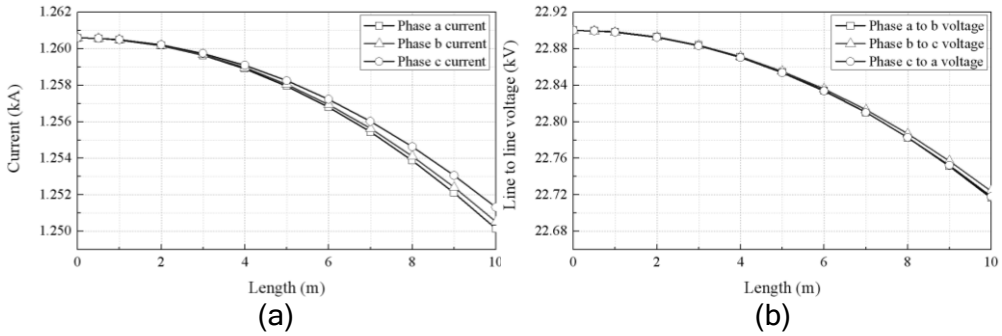

Figure 3. (a) The Current Imbalance of the Tri-axial HTS Cable; (b) the Line to Line Voltage Imbalance of the Tri-axial HTS Cable

3.2. Equivalent Circuit Model

The tri-axial HTS cable core was modeled to analyze the AC loss and electro-magnetic characteristics using *COMSOL multiphysics*. Approximation of the Maxwell equation in the H-field model of the COMSOL was used to consider non-linear electric-current density (E-J) characteristics of a superconductor. As shown in Figure 4(a), the model is a quarter of a symmetrical model of the cable and a detailed model of the 2G YBCO HTS wire. The magnetic fields of the cable are a circular orientation relative to a cross-section of the each phase and the HTS wires as shown in Figure 4(b). According to magnitude of operating current, the AC loss of the tri-axial HTS cable is shown in Figure 4(c).

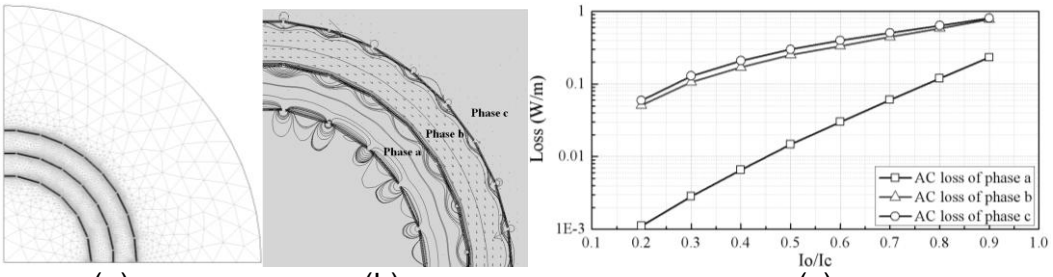

Figure 4. (a) The Quarter of a Symmetrical Model of the Tri-axial HTS Cable (b) the Magnetic Field Analysis Result of the Tri-axial HTS Cable; (c) the AC Loss of the Tri-axial HTS Cable

4. Conclusions

In this paper, a tri-axial HTS cable was designed to consider the voltage level and power capacity of the cable. Inductances and capacitances of the cable were calculated to resolve the inherent imbalance in the three-phase currents. The designed cable has the imbalance ratio of the three-phase currents about 0.09% in the case of the 10 km length cable but this imbalance ratio is negligible in a distribution class power system. When a transport current is rated operating current, the AC loss of each phase is 0.041 W/m, 0.374 W/m, and 0.439 W/m, respectively.

Compared with the triad co-axial HTS cable of 22.9 kV, 50 MVA, the designed tri-axial HTS cable core has the advantage of using only 56% of the number of HTS wire because the HTS shield of each phase is not required for the tri-axial HTS cable. The tri-axial HTS cable is economically feasible because of the amount of HTS wires used as compared with other types of HTS cable. Using this design results, the tri-axial HTS cable core will be fabricated and tested in the near future.

Acknowledgements

This work was supported by the Power Generation & Electricity Delivery of the Korea Institute of Energy Technology Evaluation and Planning (KETEP) grant funded by the Korea government Ministry of Knowledge Economy (No. 20111020400010).

References

[1] T. Hamajima, N. Hu, N. Ozcivan, S. Soeda, T. Yagai and M. Tsuda, IEEE Trans. Appl. Supercond., vol. 19, **(2009)**, pp. 1748.
[2] P. W. Fisher, M. J. Cole, J. A. Demko, C. A. Foster, M. J. Gouge, R. W. Grabovickic, J. W. Lue, J. P. Stovall, D. T. Lindsay, M. L. Roden and J. C. Tolbert, IEEE Trans. Appl. Supercond., vol. 13, **(2003)**, pp. 1938.
[3] M. A. Young, M. J. Gouge, M. O. Pace, J. A. Demko, R. C. Duckworth, J. W. Lue and Aly Fathy, IEEE Trans. Appl. Supercond., vol. 15, **(2005)**, pp. 1751.
[4] T. Hamajima, T. Yagai and M. Tsuda. IEEE Trans. Appl. Supercond., vol. 16, **(2006)**, pp. 1586.
[5] N. Hu, M. Toda, A. N. Ozcivan, T. Yagai, M. Tsuda and T. Hamajima, Physica C 470, **(2010)**, pp. 1584.
[6] T. Hamajima, A.N. Ozcivan, K. Shimoyama, S. Soeda, N. Hu, T. Yagai and M. Tsuda, Electronics and Communications in Japan, vol. 94, **(2011)**, pp. 51.
[7] K. Sim, S. Kim, J. Cho, D. Kim, C. Kim, H. Jang, S. Sohn and S. Hwang, Physica C 468, **(2008)**, pp. 2018.
[8] S. Kim, K. Sim, J. Cho, H.M. Jang and M. Park, IEEE Trans. Appl. Supercond., vol. 20, **(2010)**, pp. 2130.
[9] R. Brambilla, F. Grilli and L. Martini, Supercond. Sci. Technol., vol. 20, **(2007)**, pp. 16.
[10] P. Sharma, International Journal of Energy, Information, and Communications, vol. 1, **(2010)**, pp. 49.
[11] D. -J. Kang and S. Park, International Journal of Energy, Information, and Communications, vol. 1, **(2010)**, pp. 64.
[12] D. Miyagi, Y. Yunnoki, M. Umabuch, N. Takahashi and O. Tsukamoto, Physica C 468, **(2008)**, pp. 1743.
[13] S. P. Ashworth, M. Suenaga, Physica C 329, **(2000)**, pp. 149.

Authors

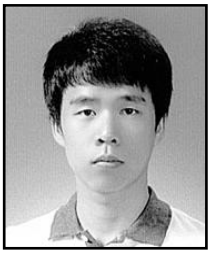

Sung-Kyu Kim

Sung-Kyu Kim was born in Korea, on February 3, 1986. He received the B.S. degree in electrical engineering from Changwon National University, Changwon, Korea, in 2008.

Currently, he is pursuing the M.S. degree in the field of superconducting power transmission cable.

Sun-Kyoung Ha

Sun-kyoung Ha was born in Korea, on September 18, 1989. She received the B.S. degree in energy and electrical engineering from Uiduk University, Gyeongju, Korea, in 2012.

Currently, she is pursuing the M.S. degree in the field of superconducting power transmission cable.

Minwon Park

Minwon Park was born in Korea, on February 12, 1970. He received the M.S. degree in electrical engineering from Changwon National University, Changwon, Korea, in 1997, and the M.S. and the Ph.D. degrees in electrical engineering from Osaka University, Osaka, Japan, in 2002.

Since 2004, he has been a professor in the Changwon National University, Changwon, Korea.

In-Keun Yu

In-Keun Yu was born in Korea, on February 18, 1954. He received the M.S. and Ph.D. degrees in electrical engineering from Hanyang University, Seoul, Korea in 1983 and 1986, respectively.

Since 1988, he has been a professor in the Changwon National University, Changwon, Korea.

Sangjin Lee

Sangjin Lee was born in Korea, on March 3, 1962. He received the M.S. and Ph.D. degrees in electrical engineering from Yonsei University, Seoul, Korea in 1991 and 1995, respectively.

Currently, he is a professor in the Uiduk University, Gyeongju, Korea.

Kideok Sim

Kideok Sim was born in Korea, on February 1, 1973. He received the M.S. and Ph.D. degrees in electrical engineering from Yonsei University, Seoul, Korea in 1999 and 2011, respectively.

Currently, he is a researcher in the Korea Electrotechnology Research Institute (KERI), Changwon, Korea.